Chem. Res. Chin. Univ., 2016, 32(4), 674—677 doi: 10.1007/s40242-016-5490-2

Chemical Evolution of $LiCoO_2$ and $NaHSO_4 \cdot H_2O$ Mixtures with Different Mixing Ratios During Roasting Process

WANG Dahui[1*], WEN Hao[1], CHEN Huaijing[2], YANG Yujiao[1] and LIANG Hongyan[1]

1. State Key Laboratory of Advance Processing and Recycling of Nonferrous Metals,

2. College of Science, Lanzhou University of Technology, Lanzhou 730050, P. R. China

Abstract Mixtures of $NaHSO_4 \cdot H_2O$ and $LiCoO_2$ extracted from spent lithium-ion batteries were prepared with molar ratios of 1:1, 1:2 and 1:3. The chemical evolution of the $LiCoO_2$ and $NaHSO_4 \cdot H_2O$ mixtures during the roasting process was investigated by means of thermogravimetric analysis and differential scanning calorimetry (TG-DSC), X-ray diffraction(XRD), scanning electron microscopy(SEM), and X-ray photoelectron spectroscopy (XPS). The results show that the chemical reactions in the $LiCoO_2$ and $NaHSO_4 \cdot H_2O$ mixtures proceed during the roasting process. The Li element in the product of the roasting process is in the form of $LiNa(SO_4)$. With the increase of the proportion of $NaHSO_4 \cdot H_2O$ in the mixtures, the Co element evolves as follows: $LiCoO_2 \rightarrow Co_3O_4 \rightarrow Na_6Co(SO_4)_4 \rightarrow Na_2Co(SO_4)_2$. The roasting products exhibit dense structures and irregular shapes, and the bonding energy of Co increases.

Keywords Spent lithium-ion battery; $LiCoO_2$; Sulfating roasting; Chemical evolution

1 Introduction

Lithium-ion batteries(LIBs) are extensively used in portable devices and electric vehicles because of their favorable characteristics, including high power and energy density, high potential, long storage life, and low self-discharge efficiency, compared with Ni-Cd or Ni-MH batteries[1—4]. The average service lifetime of LIBs is 1—3 year, and vast quantities of spent LIBs are considered as waste. The concentrations of metals of cobalt, copper, lithium, and aluminum in spent LIBs are higher than those in natural ores[5]. Therefore, recycling of spent LIBs is considered as an effective way to address the shortage of natural resources and to prevent environmental pollution[6—8].

The existing recycling processes of spent LIBs, which are currently operated in industrial or laboratory scale around the world, can be divided into three types: pyrometallurgy[9], hydrometallurgy[10], and biometallurgy[11—13]. Companies, such as Umicore(Belgium), Xstrata Nickel(Canada), S.N.A.M(France), and Sony-Sumitomo(Japan) have used pyrometallurgy as their main recycling process for spent LIBs[14]. Co is fully recovered in the form of alloy at high temperature. Other metals are easily vaporized(*i.e.*, ignoble metals, such as Li and Al), consequently forming slag or flue dust[15]. Pyrometallurgical processes are often associated with high gas emissions and require stringent gases filtration standards. In hydrometallurgical process, the active material, $LiCoO_2$, of spent LIBs has been first extracted by simply cutting steel cases. Then, $LiCoO_2$ could be separated from the Al current collectors by direct dissolution into an acid[16] or alkaline solution[17], organic solvent treatment[18], ultrasonic washing[19], thermal treatment[20], or vacuum pyrolysis[21], which could be followed by acid leaching. H_2SO_4, HCl, and HNO_3 are often used as leaching agents to extract Li and Co metals in the active material, $LiCoO_2$[22]. In general, an additive, such as H_2O_2 is required to obtain high dissolution efficiency[17]. However, Cl_2, SO_3, or NO_x are released during the concentrated acid leaching process. The acid obtained after leaching is a threat to the environment and human health. Li *et al*.[23] reported a hydrometallurgical process for the recovery of Co from spent LIBs by organic acid leaching. After acid leaching, the metal ions in the resultant solution can be recovered by chemical precipitation[16], solvent extraction[24], chemical replacement[25], crystallization[17], or electrochemical methods[26]. Biometallurgical processes have been employed to recycle the active material from spent LIBs[11—13]. However, the treatment period is long and the bacteria required are difficult to incubate. Li *et al*.[27] reported the recovery of Li and Co from spent LIBs by roasting spent $LiCoO_2$ with ammonium sulfate. All the Li ions could be leached out from roasted residue with a mixed solution containing ammonia and ammonium sulfate.

In the current study, we reported a novel way to recycle Li and Co from $LiCoO_2$ extracted from spent LIBs to obtain lithium sulfate and cobalt sulfate by roasting the mixtures of

*Corresponding author. E-mail: wangdh@lut.cn

Received December 16, 2015; accepted March 15, 2016.

Supported by the National Natural Science Foundation of China(No.51264027) and the National Basic Research Program of China(No.2012CB722806).

$LiCoO_2$ and $NaHSO_4·H_2O$. Chemical evolution characteristics of the mixtures under different roasting conditions were studied with the help of TG-DSC, XRD, SEM, and XPS.

2 Experimental

The spent LIBs(ICP083448 size battery) were employed in this study. First, the batteries were fully discharged to prevent self-ignition, and then manually dismantled to remove the plastic and steel cases. Also, the anodes and cathodes were uncurled and separated. *N*-Methyl-2-pyrrolidone(NMP) was used as a solvent to separate the experimental material, $LiCoO_2$, from the cathodes. Sodium bisulfate($NaHSO_4·H_2O$, CP grade) was used during the experimental process. The mixtures of $LiCoO_2$ and $NaHSO_4·H_2O$ with different mixing ratios were weighed and mixed completely using mortar. Then, the mixtures were transferred to a ceramic crucible and roasted at preset temperature for 0.5 h in a muffle furnace(model KSL-1100X-S). To determine the chemical changes of the mixtures during the roasting process, thermogravimetric(TG) analysis and differential scanning calorimetry(DSC) were conducted at a heating rate of 10 °C/min from 25 °C to 600 °C on a simultaneous thermal analyzer(model STA 449F3). Phase identification of $LiCoO_2$ extracted from the spent LIBs and the roasting products was performed on an X-ray diffraction(XRD) instrument(model D/max-2400) with Cu *Kα* radiation at 30 mA and 30 kV. Scanning electron microscopy(model JSM-6701F) was used to analyze the morphology of the roasting products. XPS measurements were carried out on an X-ray photoelectron spectrometer(model ESCALAB 250Xi) using Al *Kα* X-rays with energy of 1486.6 eV.

3 Results and Discussion

3.1 TG-DSC Analysis

The thermal behavior of $LiCoO_2$, $NaHSO_4·H_2O$, and the mixtures of $LiCoO_2$ and $NaHSO_4·H_2O$ with molar ratios of 1:1, 1:2, and 1:3, respectively, were analyzed *via* TG and DSC measurements. The results are presented in Fig.1. As seen from Fig.1(A), for $LiCoO_2$, there is no obvious weightlessness platform in the temperature range of 25—600 °C. Slight weightlessness and endothermic/exothermic phenomenon at the corresponding temperature are closely related to the minute amounts of impurities, such as carbon powder. These impurities come from $LiCoO_2$ can be recovered from the spent LIBs. As seen from the TG curve of Fig.1(B), there are four obvious weightlessness platforms in the temperature range of 25—600 °C, and three endothermic peaks in the corresponding DSC curves. The loss of adsorbed water is shown in the first platform of TG curve, and the loss of crystal water can be observed in the second stage. When the temperature rises to 350—450 °C, the third weightlessness platform appears. This indicates that $NaHSO_4$ has been decomposed and H_2O and $Na_2S_2O_7$ are formed. With the further increase in temperature, the weightlessness rate increases. This shows that $Na_2S_2O_7$ has been transformed to Na_2SO_4 and H_2O. Compared with Fig.1(A) and (B), the TG-DSC curves of the mixtures of $LiCoO_2$ and $NaHSO_4·H_2O$ with different molar ratios are obviously different in terms of weightlessness platform, weightlessness rate, and endothermic peak[Fig.1(C)—(E)]. These differences indicate that chemical reactions have taken place when roasting the mixture samples of $LiCoO_2$ and $NaHSO_4·H_2O$. The TG curves of the mixture samples of $LiCoO_2$ and $NaHSO_4·H_2O$ with molar ratios of 1:1, 1:2, and 1:3 show obvious weightlessness phenomenon, and that the corresponding DSC curves have strong endothermic peak at around 100—200 °C. With the increase of the molar ratio of $NaHSO_4·H_2O$ in the mixture sample of $LiCoO_2$ and $NaHSO_4·H_2O$, the weightlessness rate also increases. In the temperature range of 200—400 °C, the weightlessness phenomenon appears again; however, the weightlessness rate is significantly lower than the

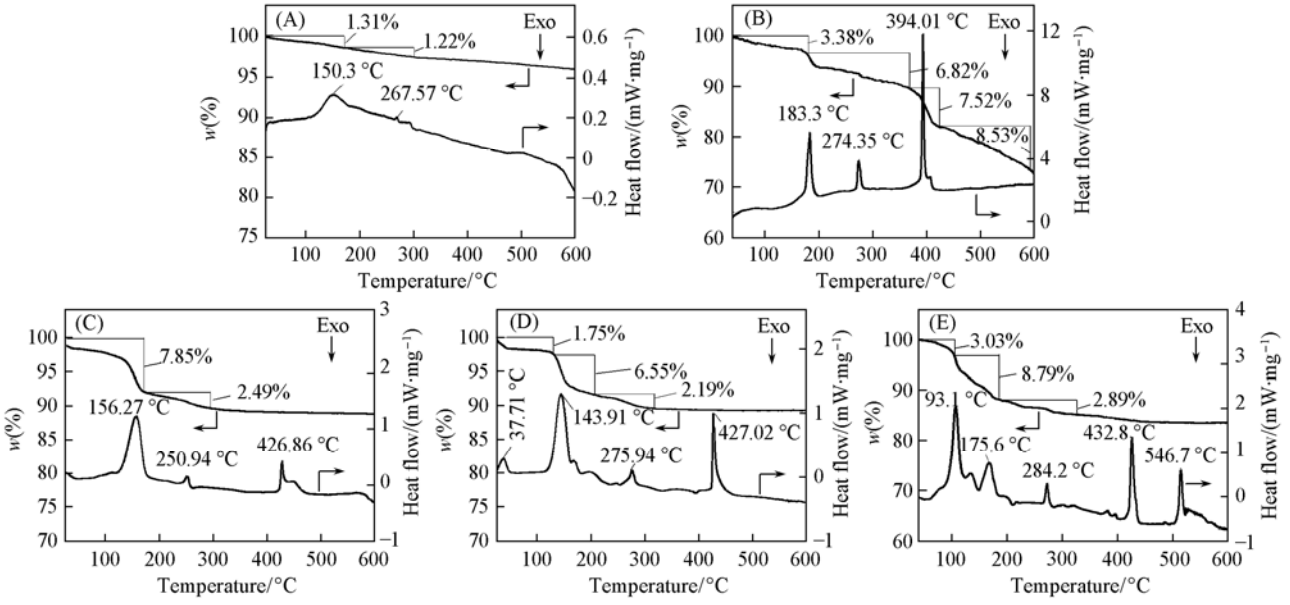

Fig.1 TG-DSC curves of $LiCoO_2$(A), $NaHSO_4·H_2O$(B) and the mixtures of $LiCoO_2$ and $NaHSO_4·H_2O$ with molar ratios of 1:1(C), 1:2(D) and 1:3(E)

roasting temperature within the range of 100—200 °C, in which the three samples have a small endothermic peak. In the temperature range of 400—600 °C, no weightlessness phenomenon occurs; however, there are three obvious endothermic peaks in the corresponding DSC curves. From 500 °C to 600 °C, the mixture sample of $LiCoO_2$ and $NaHSO_4·H_2O$ with a molar ratio of 1:3 has an endothermic peak.

3.2 XRD Analysis

Fig.2(A) shows the XRD pattern of the $LiCoO_2$ powder recovered from the spent LIB. The main component of the $LiCoO_2$ powder is $LiCoO_2$ phase, the peak shape of which is sharp and symmetrical, whereas the peak width at half height is narrow. The crystallinity of the $LiCoO_2$ powder is relatively high. In addition, there is a small amount of Co_3O_4 found in the $LiCoO_2$ powder. The appearance of Co_3O_4 is related to Li_xCoO_2 (x<1), which can be decomposed into $LiCoO_2$, Co_3O_4, and O_2[17,18]. Fig.2(B)—(D) show the XRD patterns of the mixtures of $LiCoO_2$ and $NaHSO_4·H_2O$ with molar ratios of 1:1, 1:2, and 1:3 roasted at 600 °C for 0.5 h. Comparing Fig.2(B)—(D) with Fig.2(A), the characteristic diffraction peaks of $LiCoO_2$ in the roasted products completely disappear. When the mixed molar ratio of $LiCoO_2$ and $NaHSO_4·H_2O$ is 1:1, the phase composition of the roasted products becomes $LiNa(SO_4)$ and Co_3O_4. On the other hand, when the mixed molar ratio of $LiCoO_2$ and $NaHSO_4·H_2O$ is 1:2, the phase composition of the roasted products becomes $LiNa(SO_4)$, Co_3O_4 and $Na_6Co(SO_4)_4$. When the mixed molar ratio of $LiCoO_2$ and $NaHSO_4·H_2O$ is 1:3, the phase composition of the roasted products becomes $LiNa(SO_4)$, $Na_6Co(SO_4)_4$, and $Na_2Co(SO_4)_2$.

These results show that, in the roasted products, the Li element is present in the form of $LiNa(SO_4)$, whereas the form of Co element is closely related to the proportion of $NaHSO_4·H_2O$ in the $LiCoO_2$ and $NaHSO_4·H_2O$ mixture. With the increase of the ratio of $NaHSO_4·H_2O$, the Co element evolves as follows: $LiCoO_2 \rightarrow Co_3O_4 \rightarrow Na_6Co(SO_4)_4 \rightarrow Na_2Co(SO_4)_2$.

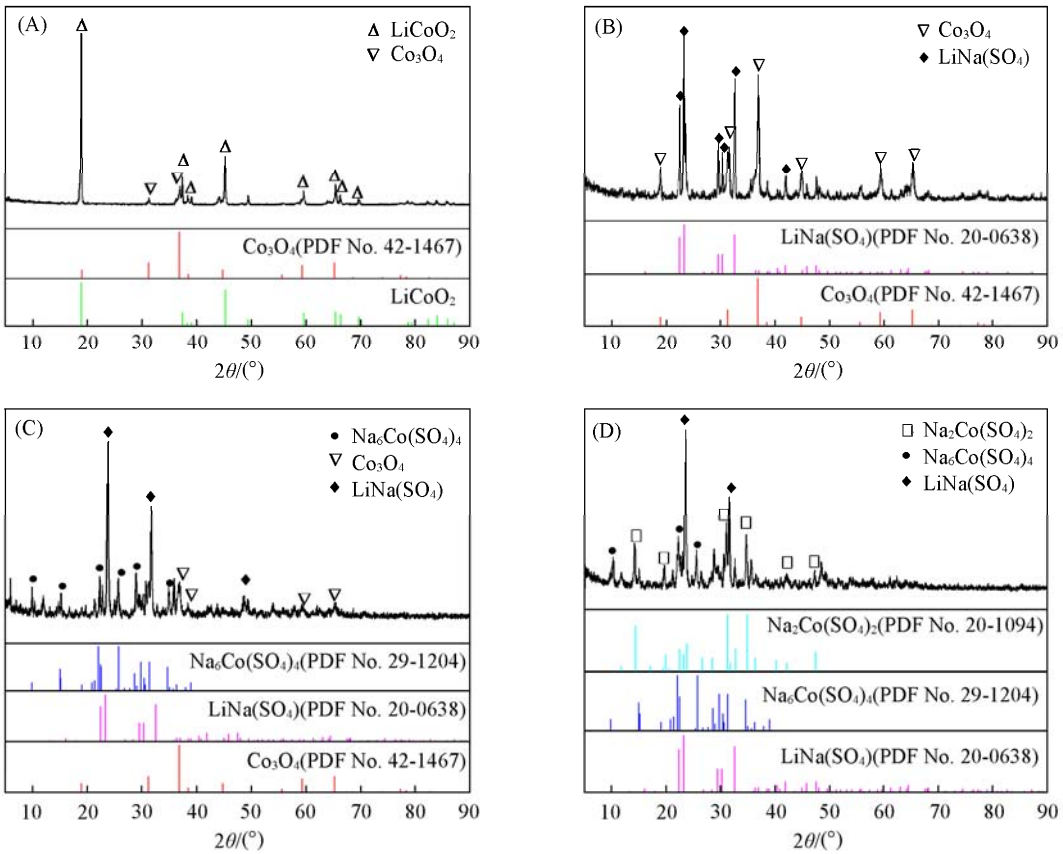

Fig.2 XRD patterns of $LiCoO_2$(A), the mixture samples of $LiCoO_2$ and $NaHSO_4·H_2O$ with molar ratios of 1:1(B), 1:2(C) and 1:3(D) roasted at 600 °C for 0.5 h

3.3 SEM Analysis

Fig.3(A)—(C) show the SEM images of the mixture samples of $LiCoO_2$ and $NaHSO_4·H_2O$ with molar ratios of 1:1, 1:2, and 1:3 roasted at 600 °C for 0.5 h, showing the massive and dense structure of the particles of the roasted products. The distribution of these particles is not uniform and the shapes are irregular. The powder particles cannot be observed.

3.4 XPS Analysis

Fig.4 shows the XPS patterns of Co_{2p} from $LiCoO_2$ and the mixture samples of $LiCoO_2$ and $NaHSO_4·H_2O$ with the molar ratios of 1:1, 1:2, and 1:3 roasted at 600 °C for 0.5 h. As shown in Fig.4, the bonding energy of Co element in the roasted products is higher than that of $LiCoO_2$. With the increase in the ratio of $NaHSO_4·H_2O$, the bonding energy of Co

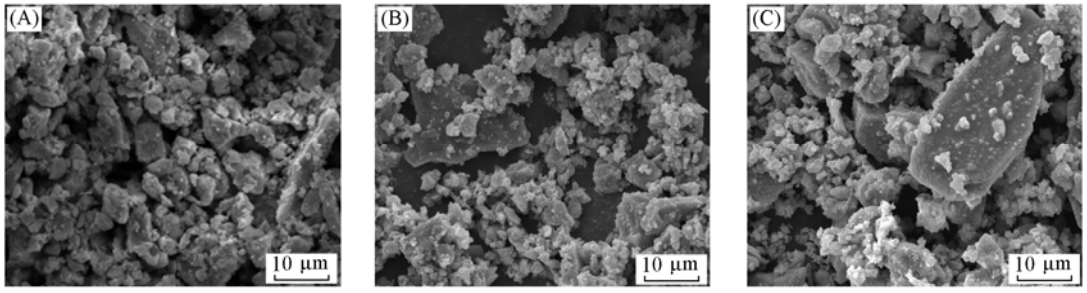

Fig.3 SEM images of the mixture samples of $LiCoO_2$ and $NaHSO_4·H_2O$ with molar ratios of 1:1(A), 1:2(B) and 1:3(C) roasted at 600 °C for 0.5 h

element also increases. This result is closely related to the changes in the form of Co element in the roasted products. Comparing the XPS pattern of Co_{2p} from the $LiCoO_2$(Fig.4 curve *a*), the peak intensities of Co_{2p} from the roasted samples(Fig.4 curves *b*—*d*) are decreased, while the peaks' shape is widened. This result indicates that the diversity of the valence states of Co element can result in the superposition of the Co peaks of different valence states. If the surface of the samples is covered by other substances without Co, the signal intensity of Co element will be reduced.

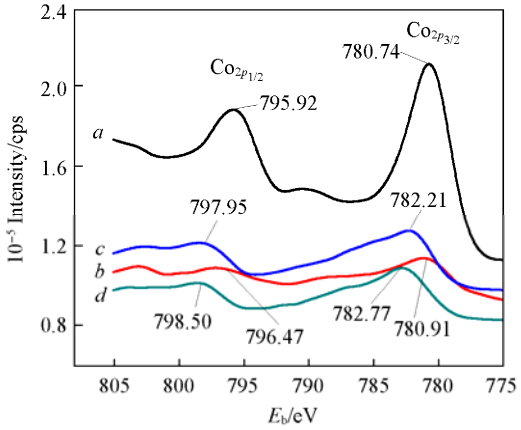

Fig.4 XPS patterns of Co_{2p} from $LiCoO_2$(*a*) and the mixture samples of $LiCoO_2$ and $NaHSO_4·H_2O$ with molar ratios of 1:1(*b*), 1:2(*c*) and 1:3(*d*) roasted at 600 °C for 0.5 h

4 Conclusions

The chemical reactions proceeded during the roasting process of the $LiCoO_2$ and $NaHSO_4·H_2O$ mixtures. The Li element in all the roasted products was present in the form of $LiNa(SO_4)$. The form of Co was closely related to the proportion of $NaHSO_4·H_2O$ in the mixtures. With the increase of $NaHSO_4·H_2O$, the Co element evolved as follows: $LiCoO_2 \rightarrow Co_3O_4 \rightarrow Na_6Co(SO_4)_4 \rightarrow Na_2Co(SO_4)_2$. Moreover, the particles of the roasted products had dense structures with irregular shapes. The bonding energy of the Co element increased with the increase of the ratio of $NaHSO_4·H_2O$.

References

[1] Etacheri V., Marom R., Elazari R., Salitra G., Aurbach D., *Energy Environ Sci.*, **2011**, *4*, 3243

[2] Bruno S. B., Hassoun J., Sun Y. K., *Energy Environ Sci.*, **2011**, *4*, 3287

[3] Jiang X., Shi N. N., Zhang Y., Cheng K., Ye K., Wang G. L., Cao D. X., *Chem. J. Chinese Universities*, **2015**, *36*(4), 739

[4] Feng G. J., Xun R. Q., Tang Z. Y., Ai H. Q., *Chem. J. Chinese Universities*, **2007**, *28*(8), 1532

[5] Dorella G., Mansur M. B., *J. Power Sources*, **2007**, *170*, 210

[6] Zeng X. L., Li J. H., *J. Hazard Mater.*, **2014**, *271*, 50

[7] Grimes S. M., Donaldsonb J. D., Chaudhary A. J., Hassan M. U., *Environ. Sci. Technol.*, **2000**, *34*(19), 4128

[8] Kang D. H. P., Chen M., Ogunseitan O. A., *Environ. Sci. Technol.*, **2013**, *47*(10), 5495

[9] Paulino J. F., Busnardo N. G., Afonso J. C., *J. Hazard Mater.*, **2008**, *150*(3), 843

[10] Shin S. M., Kim N. H., Sohn J. S., Yang D. H., Kim Y. H., *Hydrometallurgy*, **2005**, *79*(10), 172

[11] Mishra D., Kim D., Ralph D. E., Ahn J., Rhee Y., *Waste Manag.*, **2008**, *28*, 333

[12] Zeng G., Deng X., Luo S., Luo X., Zou J., *J. Hazard Mater.*, **2012**, *199*/*200*, 164

[13] Xin B., Zhang D., Zhang X., Xia Y., Wu F., Chen S., Li L., *Bioresource Technol.*, **2009**, *100*, 6163

[14] Wang H. G., Friedrich B., *J. Sustain. Metall.*, **2015**, *1*, 168

[15] Georgi-Maschler T., Friedrich B., Weyhe R., Heegn H., Rutz M., *J. Power Sources*, **2012**, *207*(6), 173

[16] Castillo S., Ansart F., Laberty-Robert C., Portal J., *J. Power Sources*, **2002**, *112*(1), 247

[17] Chen L., Tang X., Zhang Y., Li L., Zeng Z., Zhang Y., *Hydrometallurgy*, **2011**, *108*(1), 80

[18] Lain M., *J. Power Sources*, **2001**, *97*(3), 736

[19] Li L., Lu J., Ren Y., Zhang X. X., Chen R. J., Wu F., Amine K., *J. Power Sources*, **2012**, *218*(12), 21

[20] Li J. H., Zhong S. W., Xiong D. L., Chen H., *Rare Metals*, **2009**, *28*(4), 328

[21] Sun L., Qiu K., *Waste Manag.*, **2012**, *32*(8), 1575

[22] Granata G., Moscardini E., Pagnanelli F., *J. Power Sources*, **2012**, *206*, 393

[23] Li L., Ge J., Chen R., Wu F., Chen S., Zhang X., *Waste Manag.*, **2010**, *30*(12), 2615

[24] Nan J. M., Han D. M., Zuo X. X., *J. Power Sources*, **2005**, *152*(1), 278

[25] Li J., Li X., Hu Q., Wang Z., Zheng J., Wu L., Zhang L., *Hydrometallurgy*, **2009**, *99*(1/2), 7

[26] Lupi C., Pasquali M., *Miner. Eng.*, **2003**, *a16*(6), 537

[27] Li D. F., Wang C. Y., Yin F., Chen Y. Q., Jie X. W., Yang Y. Q., Wang J., *Chin. J. Process Eng.*, **2009**, *19*(2), 264